Effect of Axial Potential Distribution of Carbon Fiber on the Interfacial Performance of Carbon Fiber/Epoxy Composites in Anodizing

Xubo ZHANG [1, 2], Siyuan TIAN [1, 2], Hang SHU [1, 2], Yu WANG [1, 2 *], Lianghua XU [1, 2]

[1] *Beijing University of Chemical Technology, 15, North Third Ring Road East, Chaoyang District, Beijing 100029, China*
[2] *Key Laboratory of Carbon Fiber and Functional Polymer, Ministry of Education, 15, North Third Ring Road East, Chaoyang District, Beijing, China*

http://doi.org/10.5755/j02.ms.43439

Received 27 October 2025; accepted 18 December 2025

Anodic oxidation of carbon fibers has attracted considerable attention for interfacial modification of composites due to its advantages of continuous processing capability and uniform surface modification. However, the mechanism by which the axial potential distribution along carbon fibers affects surface modification behavior and interfacial performance remains unclear. In this study, the axial potential distribution of carbon fibers during anodic oxidation was investigated by regulating the electrode potential, and its effect on the interfacial properties of carbon fiber/epoxy composites was analyzed. The results show that: 1) the axial potential of carbon fibers decreases progressively with increasing distance from the anode plate. This decay is caused by the combined effects of the intrinsic resistance of the fibers and the conductive loss of the electrolyte, which consequently limits the effective region of the electrochemical reaction; 2) within the effective reaction region, a moderate increase in the fiber potential can significantly improve the interfacial performance of the composites, whereas an excessively high potential leads to degradation of interfacial properties; 3) a smoother and more uniform potential distribution is more favorable for achieving strong interfacial bonding.
Keywords: carbon fiber, anodic oxidation, axial potential distribution, surface functional groups, interfacial properties.

1. INTRODUCTION

Polyacrylonitrile (PAN)-based carbon fibers, which combine excellent mechanical performance with lightweight characteristics, have been widely applied in aerospace, national defense, and advanced equipment manufacturing fields [1]. However, as the tensile modulus of carbon fibers increases, the degree of graphitization is enhanced, resulting in a gradual reduction of surface chemical activity. Consequently, the interfacial adhesion between the carbon fibers and polymer matrix becomes weaker, thereby limiting the overall mechanical performance of the composites [2, 3].

To improve the interfacial compatibility between carbon fibers and resin matrices, numerous surface modification techniques have been developed, including chemical vapor deposition [4], surface coating [5], plasma treatment [6], surface grafting [7, 8], and electrochemical oxidation [9 – 12]. Among these, anodic oxidation has attracted significant attention owing to its operational simplicity, continuous processing feasibility, and uniform surface modification. In this method, the carbon fibers act as the anode, and inert metals or graphite serve as the cathode. The surface oxidation of the fibers is achieved through electrochemical reactions in acidic, basic, or saline electrolytes [13].

Current research on anodic oxidation has mainly focused on the effects of process parameters – such as electrolyte type [14 – 18], current density [19 – 21], electrolyte concentration [22, 23], and treatment duration [24] – on the modification efficiency. However, the influence of axial potential distribution along the fiber direction on interfacial properties has not been systematically studied. Sun [25] established a model showing that the axial potential of carbon fibers gradually decreases and levels off with increasing treatment length, but the effects of this potential distribution on surface chemical structure and interfacial performance were not further explored.

In view of this, the present study systematically investigates the axial potential distribution of carbon fibers during anodic oxidation by regulating electrode potential. Combined with analyses of surface functional group evolution and interfacial shear performance, the coupling mechanism between potential distribution and interfacial bonding strength is revealed. This work provides both a theoretical basis and technical guidance for the optimization of electrochemical surface modification of carbon fibers.

2. EXPERIMENTAL SECTION

2.1. Materials

The carbon fibers used in this study were prepared from laboratory-made polyacrylonitrile (PAN) precursor yarns (12K) through pre-oxidation, carbonization, and graphitization processes. The resulting fibers exhibited a tensile modulus of 320 GPa, an average monofilament diameter of approximately 5.2 μm, a bundle cross-sectional area of 2.55×10^{-7} m², and a resistivity of 1.1×10^{-5} Ω·m. Analytical grade sulfuric acid used for anodic oxidation was purchased from Beijing Modern Oriental Fine Chemical

* Corresponding author: Y. Wang
E-mail: *wangy@mail.buct.edu.cn*

Co., Ltd. The E-51 epoxy resin was supplied by Shanghai Huayi Resin Co., Ltd., while the curing agent methyl tetrahydrophthalic anhydride and the accelerator aminoethylpiperazine were obtained from Beijing Chemical Factory.

2.2. Anodic oxidation process

The anodic oxidation setup is illustrated in Fig. 1 a. A platinum plate served as the anode and an alloy plate as the cathode. The electrolyte was a 0.3 wt.% sulfuric acid aqueous solution, which was circulated using a water pump to maintain continuous flow. After anodic oxidation, the carbon fibers were thoroughly rinsed with deionized water and dried. The origin of the axial coordinate was defined at the front edge of the cathode plate, with the total cathode length being 40 cm; the treatment length of the carbon fibers was determined accordingly.

2.3. Preparation of unidirectional carbon fiber/epoxy composites

Individual carbon fiber was fixed onto a specialized frame. A resin mixture was prepared by blending E-51 epoxy resin, methyl tetrahydrophthalic anhydride, and aminoethylpiperazine at a mass ratio of 100:83:1.5, followed by thorough stirring. The resin mixture was then applied onto the fiber surface using a metal needle, forming droplet-like coatings via surface tension. The samples were cured in an oven at 130 °C for 3 h. After curing, the samples were mounted into testing molds, and both ends were fixed with adhesive. Once the adhesive was completely dried, the specimens were used for interfacial shear strength (IFSS) testing.

2.4. Characterization and measurements

The electrical resistivity of the carbon fibers was measured using the four-point probe method. The current was supplied by a DC/AC source (Model 6221, Keithley, USA), and the potential was recorded using a nanovoltmeter (Model 2182A, Keithley, USA), as schematically shown in Fig. 1 c.

The axial potential of the carbon fibers during anodic oxidation was measured using a multimeter (VC9802A, VICTOR, China). Measurements were taken every 5 cm along the fiber above the cathode plate. To ensure reliable contact, the fibers were supported with glass rods during testing.

Surface morphologies of the carbon fibers were observed using a scanning electron microscope (JSM-7800F, JEOL, Japan). The samples were sputter-coated with gold to enhance conductivity prior to imaging. The accelerating voltage was 10 kV, and the distance between the sample stage and the objective lens was approximately 10 mm.

The surface chemical structure was characterized using X-ray photoelectron spectroscopy (Nexsa G2, Thermo, USA). The sample was ultrasonically cleaned before testing, and the base pressure vacuum during testing was 12.0×10^{-7}. A monochromatic Al Kα X-ray source with a photon energy of 1486.6 eV was used. with a passband energy of 100 eV for wide-scan spectra and 30 eV for high-resolution spectra.

The C 1s spectral in this study were all analyzed using Casa XPS software (UK Casa Software Ltd.), processing the range from 280 to 292 eV with a Shirley baseline. The C 1s spectra were deconvolved into five components: C=C (284.8 eV), C–C (285.5 ± 0.1 eV), C–O (286.2 ± 0.2 eV), C=O (286.9 ± 0.3 eV), and O–C=O (288.6 ± 0.2 eV).

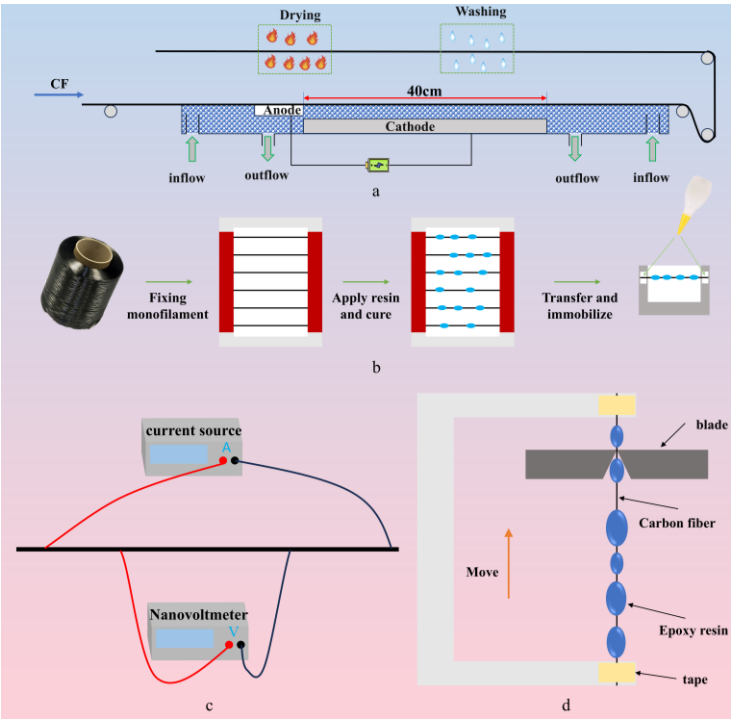


Fig. 1. Schematic diagrams of the experimental procedures: a – anodic oxidation process; b – preparation of unidirectional carbon fiber/epoxy composites; c – four-point measurement of carbon fiber resistivity; d – microdroplet debonding test for interfacial shear strength (IFSS)

The correspondence between chemical groups and binding energies was consistent with that described in the literature [22]. The fitting peak adopted an asymmetric fitting peak [26]. The proportions of different oxygen-containing functional groups on the carbon fiber surface were obtained by integrating the area.

The interfacial properties of carbon fibers were evaluated using a composite interfacial testing device (HM410, TOEI KASEI Company, Japan) through the micro-droplet debonding method to determine the interfacial shear strength (IFSS). Epoxy droplets with an embedded length of 40 – 55 μm were selected for each test. Twenty valid data points were averaged for each sample group. The IFSS was calculated according to the following equation:

$$\text{IFSS} = \frac{F_{max}}{\pi d l}, \quad (1)$$

where F_{max} is the maximum force at debonding; d is the diameter of the single carbon fiber; L is the embedded length of the epoxy resin. The schematic diagram of the testing setup is shown in Fig. 1 d.

3. RESULTS AND DISCUSSION

3.1. Axial potential distribution of carbon fibers during anodic oxidation

Fig. 2 a depicts the variation of axial potential along the carbon fiber during anodic oxidation. Both the potential magnitude and its gradient progressively decrease with increasing distance from the anode plate. The extent of potential attenuation varies under different initial electrode potentials [25]. With higher initial potentials, the axial potential decays more rapidly, indicating that both the intrinsic resistance of the carbon fiber and the conductive losses in the electrolyte contribute more significantly to potential attenuation at elevated voltages.

According to Ohm's law, the theoretical potential drop along the fiber was calculated (Fig. 2 b), and the comparison between theoretical and measured attenuation values under various initial potentials is summarized in Table 1. The measured potential attenuation is consistently greater than the theoretical value, and the discrepancy increases with initial potential. This deviation suggests that, in addition to the inherent electrical resistance of the fiber, the ionic conductivity of the electrolyte and the interfacial electrochemical reactions collectively amplify the potential loss.

Table 1. Comparison of theoretical and experimental axial potential attenuation of carbon fibers under different initial potentials

Initial potential, V	Theoretical attenuation, V	Experimental attenuation, V	Difference, V
0.83	0.10	0.20	0.10
0.99	0.16	0.31	0.15
1.24	0.21	0.42	0.21
1.44	0.23	0.46	0.23
2.05	0.26	0.51	0.25
2.70	0.51	1.02	0.51

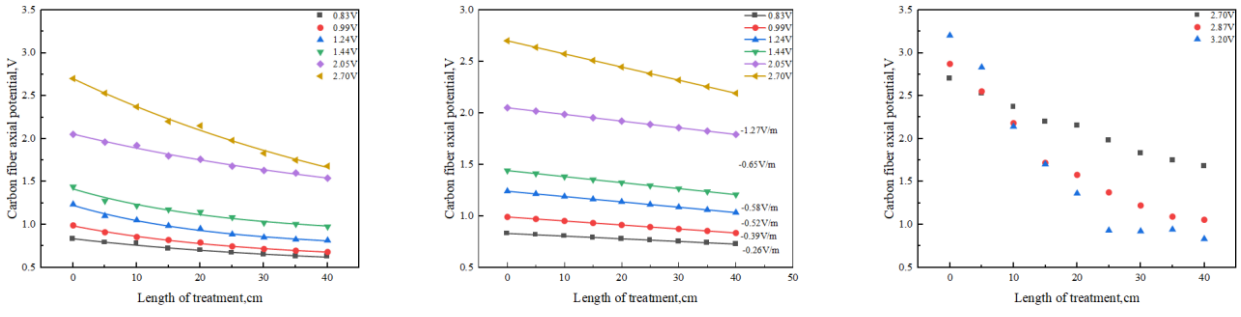
When the initial potential was further increased (Fig. 2 c), potential losses in the electrolyte intensified, causing a substantial decrease in potential in regions distant from the anode. In some cases, the local potential even fell below that of lower initial potential conditions. Such a non-uniform potential distribution narrows the effective oxidation zone and compromises the uniformity and stability of surface modification.

3.2. Effect of axial potential distribution on surface chemical structure

3.2.1. Surface chemical evolution under moderate potential (2.7 V)

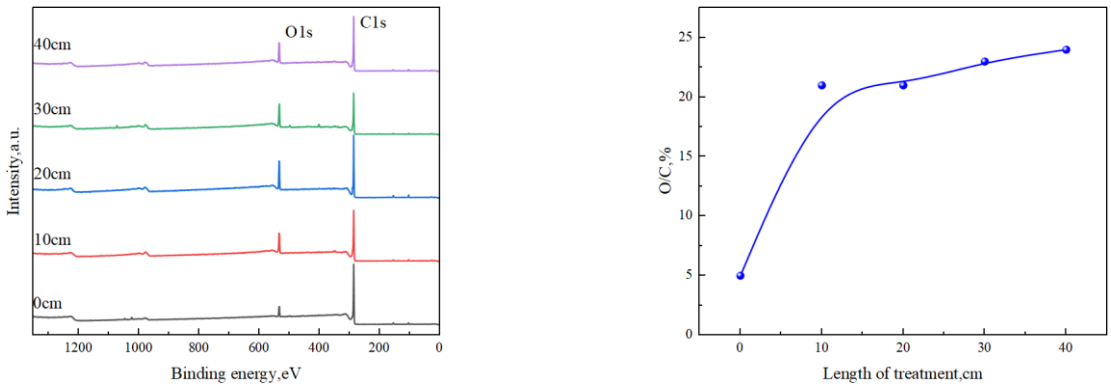
The XPS survey spectra of carbon fibers anodized at 2.7 V over different treatment lengths are shown in Fig. 3 a. The increasing intensity of the O1s peak with distance indicates a gradual enrichment of oxygen on the fiber surface (Fig. 3 b). This demonstrates that within the effective electrochemical reaction region, anodic oxidation continuously promotes the generation and accumulation of oxygen-containing functional groups [27, 28]. However, as the reaction proceeds further along the axis, the rate of oxygen accumulation slows, likely due to oxidation saturation combined with the axial potential decay.

Deconvolution of the C 1s spectra (Fig. 4) and the quantitative data summarized in Table 2 reveal that the relative contents of hydroxyl (C–O) and carboxyl (O–C=O) groups increase steadily with treatment length, whereas carbonyl (C=O) groups exhibit a rise–fall trend. This evolution is attributed to the secondary oxidation of carbonyl groups into carboxyl species during prolonged treatment. Overall, moderate potential and appropriate oxidation length facilitate the formation of abundant oxygen functionalities, enhancing the surface polarity and reactivity of carbon fibers.



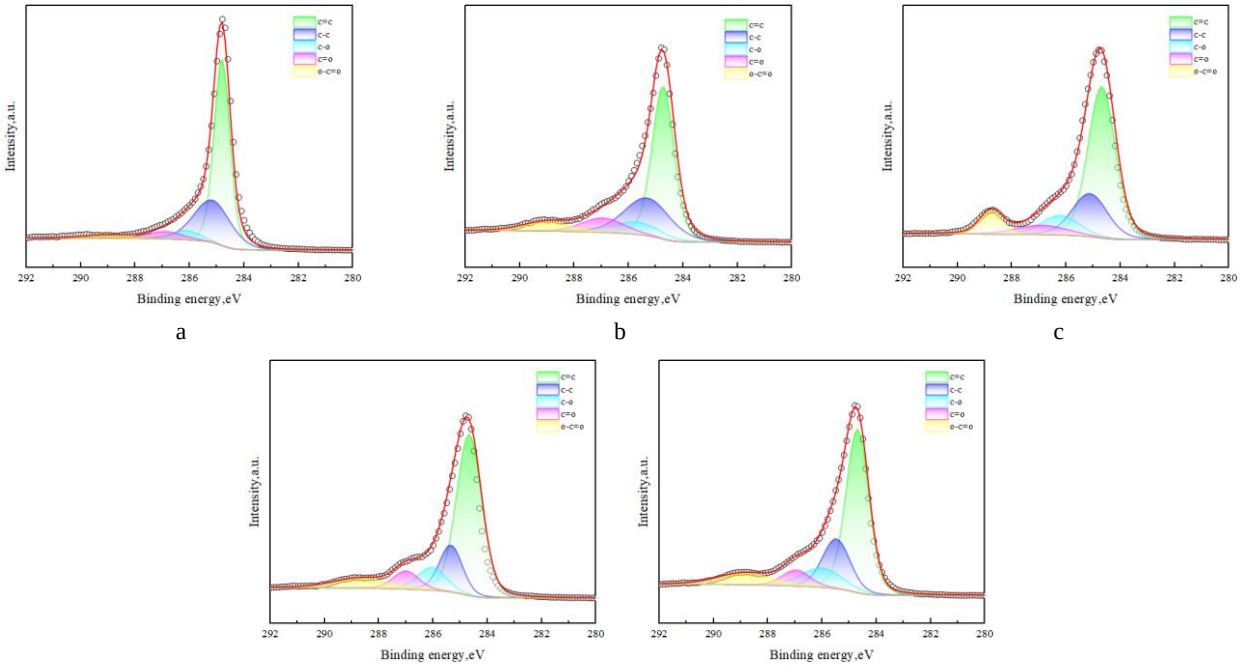
a b c

Fig. 2. Axial potetial distribution of carbon fibers during anodic oxidation: a – measured potential profiles under different initial electrode potentials; b – potential variation calculated from Ohm's law; c – at higher initial potentials



a b

Fig. 3. a – XPS survey spectra of carbon fibers anodized at 2.7 V with different treatment lengths; b – variation of the O/C atomic ratio with treatment length



a b c

d e

Fig. 4. Deconvoluted C 1s spectra of carbon fibers treated at 2.7 V over different lengths: a – 0 cm; b – 10 cm; c – 20 cm; d – 30 cm; e – 40 cm

Table 2. Relative contents of surface oxygen-containing functional groups (C–O, C=O, O–C=O) on carbon fibers treated at 2.7 V with different lengths

Length of treatment, cm	Content, %		
	C–O	C=O	O–C=O
0	1.67	1.64	0.86
10	4.95	5.15	3.67
20	5.55	3.56	3.96
30	5.64	3.96	4.64
40	6.08	3.37	4.80

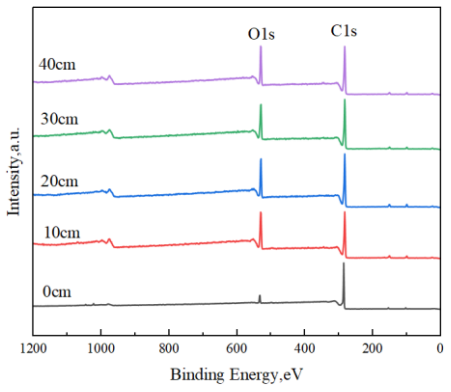
3.2.2. Surface chemical evolution under excessive potential (3.2 V)

The XPS survey spectra of carbon fibers anodized at 3.2 V over different treatment lengths are shown in Fig. 5 a, it shows that the O1s peak intensity first increases and then decreases with distance (Fig. 5 b), indicating that the oxygen concentration drops beyond a certain region. The deconvoluted C 1s spectra (Fig. 6) and content data (Table 3) demonstrate a continuous reduction in hydroxyl, carbonyl, and carboxyl contents along the fiber length.

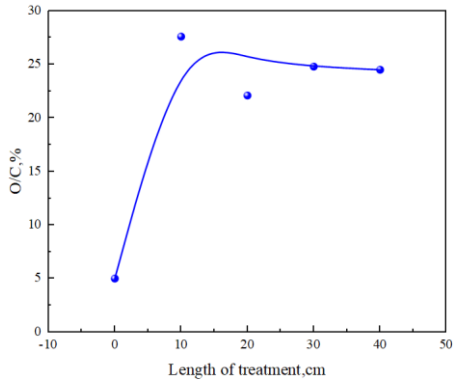
Table 3. Relative contents of oxygen-containing functional groups (C–O, C=O, O–C=O) on carbon fiber surfaces anodized at 3.2 V

Length of treatment, cm	Content, %		
	C–O	C=O	O–C=O
10	4.94	4.26	6.23
20	4.29	3.59	5.11
30	3.70	3.79	6.20
40	3.63	3.72	6.18

It suggests that excessive potential induces over-oxidation or surface layer exfoliation, which reduces the density of active functional groups and weakens the surface modification effect.



a



b

Fig. 5. a – XPS survey spectra of carbon fibers anodized at 3.2 V with different treatment lengths; b – variation of the O/C atomic ratio with treatment length

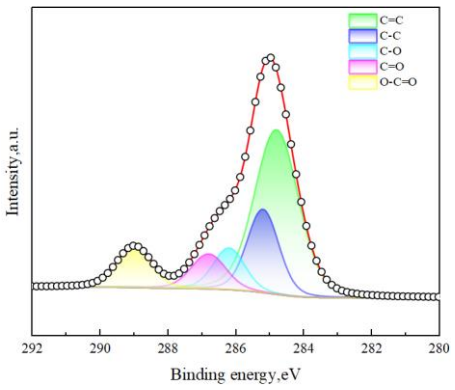
Integrating the potential distribution results with the XPS analysis indicates that anodic oxidation requires sufficient surface potential to sustain oxidation reactions. Within a moderate range, higher potential accelerates oxygen incorporation. However, excessive potential dramatically increases the reaction rate, causing severe oxidation and removal of amorphous carbon.

3.3. Effect of axial potential distribution on interfacial properties of composites

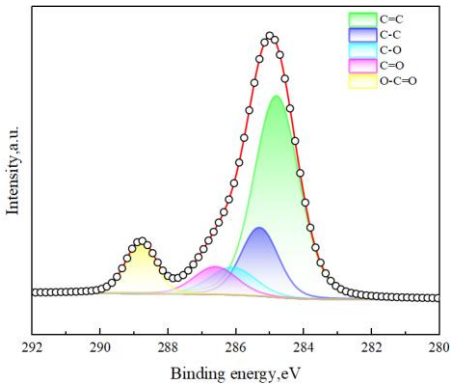
Fig. 7 presents the variation of interfacial shear strength (IFSS) of carbon fiber/epoxy composites as a function of treatment length under different initial potentials. When the initial potential is 2.7 V, the IFSS increases significantly with treatment length, reaching a 90.2 % improvement at 40 cm. Conversely, at 3.2 V, the IFSS enhancement decreases to 46.4 %, implying that excessive potential is detrimental to interfacial adhesion.

This trend correlates strongly with the evolution of surface functional groups. A moderate potential favors the formation of polar oxygen functionalities (e.g., –OH, –COOH), which enhance chemical bonding and wettability between the fiber and the resin. In contrast, over-oxidation at high potential reduces the concentration of active sites and introduces microstructural damage, weakening interfacial bonding.

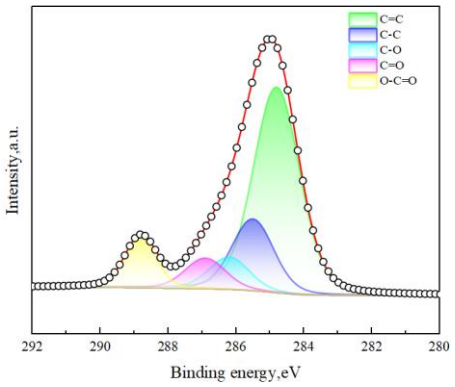
The post-debonding morphologies (Fig. 8) further support this observation. For untreated fibers, the resin droplets detach cleanly, leaving a smooth fiber surface (Fig. 8 a, b). After anodic oxidation at 2.7 V, the deboned regions become rough with substantial resin residue and higher displacement during detachment (Fig. 8 c, d), reflecting improved interfacial adhesion. At 3.2 V, however, the fiber surface appears smooth again with limited resin remnants (Fig. 8 e, f), likely due to surface exfoliation induced by over-oxidation.



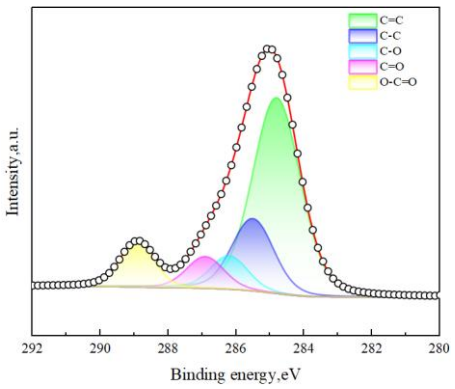
a



b

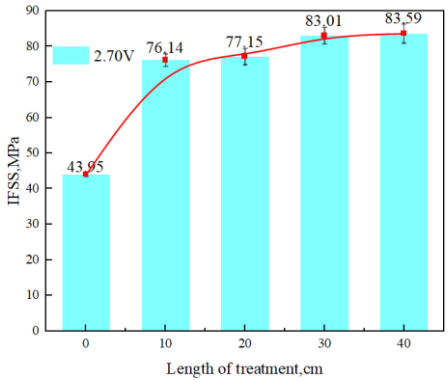


c

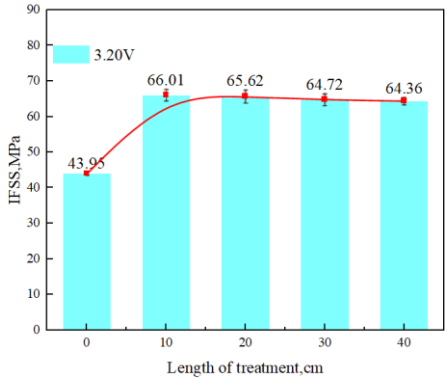


d

Fig. 6. Deconvoluted C 1s spectra of carbon fibers treated at 3.2 V with different treatment lengths: a – 10 cm; b – 20 cm; c – 30 cm; d – 40 cm



a



b

Fig. 7. Variation of interfacial shear strength (IFSS) of composites with treatment length under different initial potentials: a – 2.7 V; b – 3.2 V

The force–displacement curves obtained from microdroplet tests (Fig. 9) reveal that untreated samples exhibit brittle debonding behavior, whereas anodized fibers show larger displacement and ductile failure characteristics, confirming enhanced interfacial toughness [29 – 31].

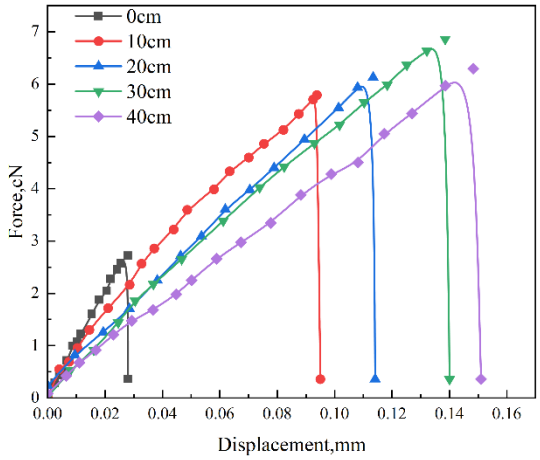


Fig. 9. Force-displacement curves of carbon fiber/epoxy microdroplets with different treatment lengths under 2.7 V

Moreover, as treatment length increases, the displacement at equivalent debonding force rises, indicating improved interfacial strength.

On a microstructural level (Fig. 10), there are two types of structures present in carbon fibers, amorphous and graphitic carbon [32, 33]. Under moderate potentials, oxidation preferentially initiates in amorphous regions, with the edges of graphitic lamellae gradually activated to form stable oxygenated groups. Under excessive potentials, the amorphous domains are excessively oxidized or even eroded, whereas the graphitic structures remain relatively intact. Consequently, the overall amount of active oxygen functional groups decreases, leading to fewer interfacial chemical bonds and reduced IFSS.

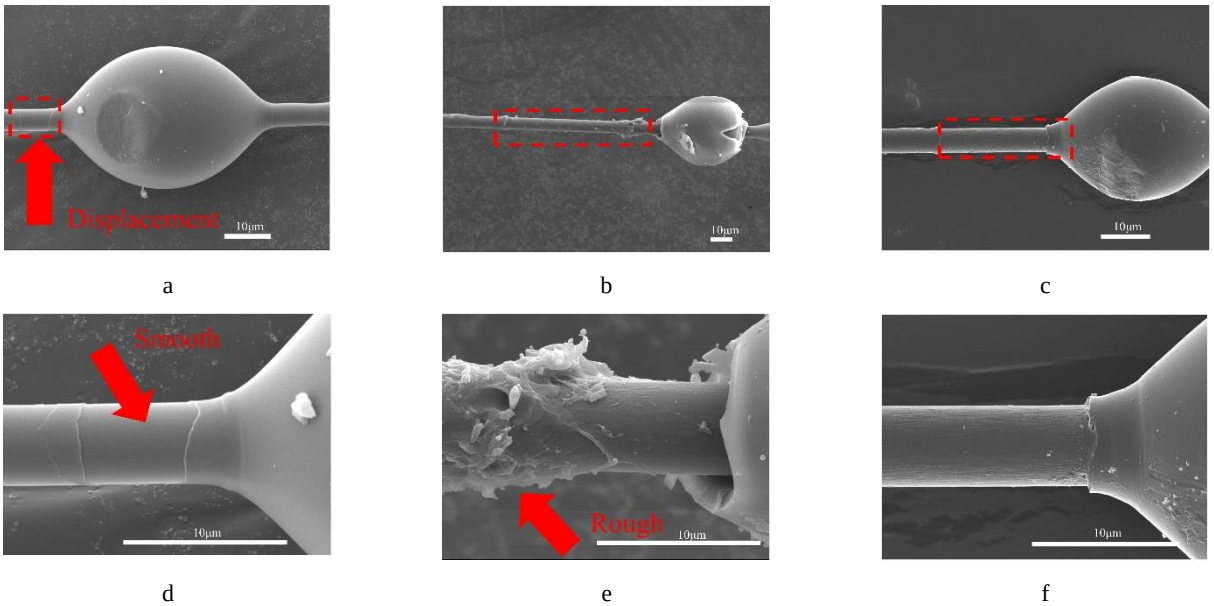


Fig. 8. Surface morphologies of carbon fibers after microdroplet debonding tests: a, b – untreated fibers; c, d – fibers treated at a moderate potential; e, f – fibers treated at an excessive potential

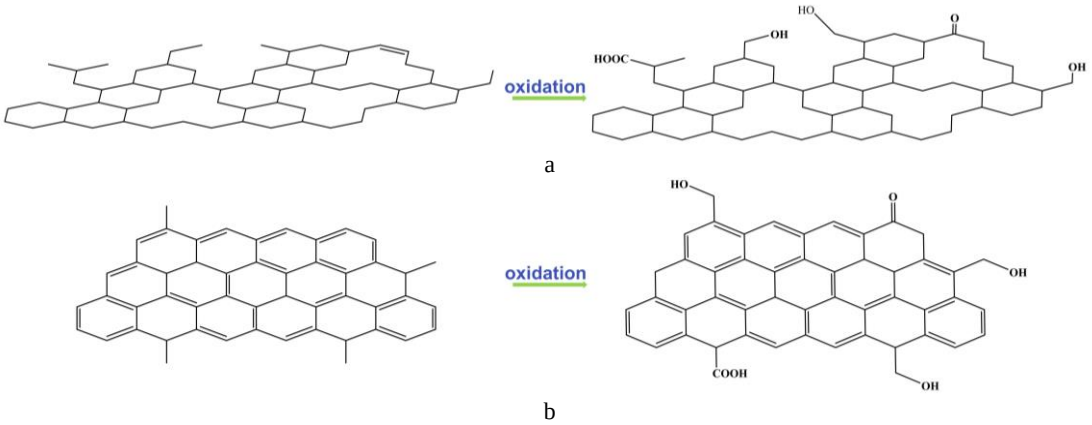


Fig. 10. Oxidation reactions occurring within the carbon fiber structure: a – amorphous carbon; b – graphitized carbon

4. CONCLUSIONS

1. The axial potential of carbon fibers decreases with increasing distance from the anode plate during anodic oxidation, primarily due to the combined effects of fiber resistance and electrolyte conductivity losses. A higher initial potential leads to a more non-uniform potential distribution and a shorter effective oxidation region.
2. Within the effective electrochemical region, a moderate anodic potential (2.7 V) facilitates the formation and accumulation of oxygen-containing functional groups, thereby enhancing fiber surface polarity. In contrast, an excessive potential (3.2 V) causes surface exfoliation and a reduction in functional group density.
3. With an optimized potential distribution, the interfacial shear strength (IFSS) of composites increases from 43.95 MPa to 83.59 MPa (an improvement of 90.2 %), and the interfacial failure mode shifts from brittle to ductile debonding. However, at high potential, the IFSS enhancement drops to 46.4 %.
4. The research results highlight that a smooth axial potential distribution coupled with a moderate anodic potential is crucial for achieving superior interfacial performance.

Acknowledgments

Thanks to the School of Materials Science and Engineering, Beijing University of Chemical Technology for providing the experimental platform.

REFERENCES

1. **Hao, L., Peng, P., Yang, F., Zhang, B., Zhang, J., Lu, X., Jiao, W., Liu, W., Wang, R., He, X.** Study of Structure–Mechanical Heterogeneity of Polyacrylonitrile-Based Carbon Fiber Monofilament by Plasma Etching-Assisted Radius Profiling *Carbon* 114 2017: pp. 317 – 323. https://doi.org/10.1016/j.carbon.2016.12.037
2. **Liu, L., Jis, C., He, J., Zhao, F., Fan, D., Xing, L., Wang, M., Wang, F., Jiang, Z., Huang, Y.** Interfacial Characterization, Control and Modification of Carbon Fiber Reinforced Polymer Composites *Composites Science and Technology* 121 2015: pp. 56 – 72. https://doi.org/10.1016/j.compscitech.2015.08.002
3. **Hung, P., Lau, K.T., Fox, B., Hameed, N., Lee, J.H., Hui, D.** Surface Modification of Carbon Fibre Using Graphene-Related Materials for Multifunctional Components. *Composites Part B: Engineering* 133 2018: 240 – 257. https://doi.org/10.1016/j.compositesb.2017.09.010
4. **Zheng, L., Wang, Y., Qin, J, Wang, X., Lu, R., Qu, C., Wang, C.** Scalable Manufacturing of Carbon Nanotubes on Continuous Carbon Fibers Surface From Chemical Vapor Deposition *Vacuum* 152 2018: pp. 84 – 90. https://doi.org/10.1016/j.vacuum.2018.03.011
5. **Zhang, T., Qi, L., Li, S., Chao, X., Tian, W., Zhou, J.** Evaluation of the Effect of PyC Coating Thickness on the Mechanical Properties of T700 Carbon Fiber Tows *Applied Surface Science* 463 2018: pp. 310 – 321. https://doi.org/10.1016/j.apsusc.2018.08.195
6. **Jang, J., Yang, H.** The Effect of Surface Treatment on the Performance Improvement of Carbon Fiber/Polybenzoxazine Composites *Journal of Materials Science* 35 (9) 2000: pp. 2297 – 2303. https://doi.org/10.1023/A:1004791313979
7. **Peng, Q., He, X., Li, Y.** Chemically and Uniformly Grafting Carbon Nanotubes Onto Carbon Fibers by Poly(amidoamine) for Enhancing Interfacial Strength in Carbon Fiber Composites *Journal of Materials Chemistry A* 22 (13) 2012: pp. 5928 – 5931. https://doi.org/10.1039/C2JM16723A
8. **Ruan, R.Y., Wang, Y., Hu, C.T.,Gao A.J., Xu L.H.** Electrode Potential Regulation of Carbon Fiber Based on Galvanic Coupling and its Application in Electrochemical Grafting *ACS Applied Materials & Interfaces* 13 (14) 2021: pp. 17013 – 17021. https://doi.org/10.1021/acsami.1c00292
9. **Osbeck, S., Bradley, R., Liu, C., Idriss, H., Ward, S.** Effect of an Ultraviolet/Ozone Treatment on the Surface Texture and Functional Groups on Polyacrylonitrile Carbon Fibres *Carbon* 49 (13) 2011: pp. 4322 – 4330. https://doi.org/10.1016/j.carbon.2011.06.005
10. **Li, J.** The Effect of Surface Modification With Nitric Acid on the Mechanical and Tribological Properties of Carbon Fiber-Reinforced Thermoplastic Polyimide Composite *Surface and Interface Analysis* 41 (9) 2009: pp. 759 – 763. https://doi.org/10.1002/sia.3089
11. **Zhang, X., Pei, X., Jis, Q., Wang, Q.** Effects of Carbon Fiber Surface Treatment on the Tribological Properties of 2D Woven Carbon Fabric/Polyimide Composites *Applied Physics A* 96 (2) 2009: pp. 535 – 545. https://doi.org/10.1007/s00339-009-5073-x
12. **Tiwari, S., Bijwe, J., Panier, S.** Tribological Studies on Polyetherimide Composites Based on Carbon Fabric With

Optimized Oxidation Treatment *Wear* 271 (9 – 10) 2010: pp. 2252 – 2260. https://doi.org/10.1016/j.wear.2010.11.052

13. **Zheng, H., Zhang, W., Li, B., Zhu, J., Wang, C., Song, G., Wu, G., Yang, X., Huang, Y., Ma, L.** Recent Advances of Interphases in Carbon Fiber-Reinforced Polymer Composites: A Review *Composites Part B: Engineering* *239* 2022: pp. 109639. https://doi.org/10.1016/j.compositesb.2022.109639
14. **Qian, X., Wang, X., Ouyang, Q., Chen, Y., Yan, Q.** Effect of Ammonium-Salt Solutions on the Surface Properties of Carbon Fibers in Electrochemical Anodic Oxidation *Applied Surface Science* 259 2012: pp. 238 – 244. https://doi.org/10.1016/j.apsusc.2012.07.025
15. **Sun, Y., Yang, C., Lu, Y.** Weak Layer Exfoliation and an Attempt for Modification in Anodic Oxidation of PAN-Based Carbon Fiber *Journal of Materials Science* 55 (6) 2020: pp. 2372 – 2379. https://doi.org/10.1007/s10853-019-04109-8
16. **Bauer, M., Beratz, S., Ruhland, K., Horn, S., Will, M.J.** Anodic Oxidation of Carbon Fibers in Alkaline and Acidic Electrolytes: Quantification of Surface Functional Groups by Gas-Phase Derivatization *Applied Surface Science* 506 2020: pp. 144947. https://doi.org/10.1016/j.apsusc.2019.144947
17. **Sun, Y., Lu, Y., Yang, C.** Stripping Mechanism of PAN-Based Carbon Fiber During Anodic Oxidation in NaOH Electrolyte *Applied Surface Science* 486 2019: pp. 128 – 136. https://doi.org/10.1016/j.apsusc.2019.05.018
18. **Fu, Y., Li, H., Cao, W.Y.** Enhancing the Interfacial Properties of High-Modulus Carbon Fiber Reinforced Polymer Matrix Composites via Electrochemical Surface Oxidation and Grafting *Composites Part A* 130 2020: pp. 105719. https://doi.org/10.1016/j.compositesa.2019.105719
19. **Qian, X., Zhi, J., Chen, L., Huang, J., Zhang, Y.** Effect of Low Current Density Electrochemical Oxidation on the Properties of Carbon Fiber-Reinforced Epoxy Resin Composites *Surface and Interface Analysis* 45 (5) 2013: pp. 937 – 942. https://doi.org/10.1002/sia.5001
20. **Qian, X., Zhang, G.Y., Wang, F.X., Heng, Y., Zhi, J.** Effect of Carbon Fiber Surface Functionality on the Moisture Absorption Behavior of Carbon Fiber/Epoxy Resin Composites *Surface and Interface Analysis* 48 (12) 2016: pp. 1271 – 1277. https://doi.org/10.1002/sia.6317
21. **Kyu, D.K., Woo, K.K., Woong, H., Bhumkeun, B., Yub, S.Y., Yun, H.B., Joo, B.K.** Effects of Increase in Ratio of Phenolic Hydroxyl Function on Carbon Fiber Surfaces by Anodic Oxidation on Mechanical Interfacial Bonding of Carbon Fibers-Reinforced Epoxy Matrix Composites *Applied Chemistry for Engineering* 27 (5) 2016: pp. 472 – 477. https://doi.org/10.14478/jpcea.27.472
22. **Xiao, J., Tian, S.Y., Zhou, H., Gao, A.J., Xu, L.H.** Construction of Polar Functional Groups on the Surface of a High-Modulus Carbon Fiber and its Effect on the Interfacial Properties of Composites *ACS Omega* 8 (32) 2023: pp. 29262 – 29269. https://doi.org/10.1021/acsomega.3c02596
23. **Huang, C., Zhang, P., Liu, Z., Sun, M., Liu, H., Sun, J., Li, B., Zhao, Y., Bao, J.** Effect of Electrochemical Anodic Oxidation Modification on the Interfacial Properties of Carbon Fiber Reinforced Polyimide Composites *Polymer Composites* 46 (3) 2025: pp. 2390 – 2403. https://doi.org/10.1002/pc.29112
24. **Hu, Y., Zhang, J., Wang, L., Cheng, F., Hu, X.** Enhancing Adherent Bond Strength of CFRP/Titanium Joints Through NaOH Anodising and Resin Pre-Coating Treatments With Optimized Anodising Conditions *Chinese Journal of Aeronautics* 37 (2) 2024: pp. 511 – 523. https://doi.org/10.1016/j.cja.2023.11.007
25. **Sun, Y., Lu, Y., Zhang, W., Yao, L., Liu, L., Yang, C.** Simulations of Potential Distribution and Efficiency Optimization in Carbon Fiber Electrochemical Oxidation *Journal of The Electrochemical Society* 165 (3) 2018: pp. E115 – E120. https://doi.org/10.1149/2.0221803jes
26. **Susi, T., Pichler, T., Ayala, P.** X-Ray Photoelectron Spectroscopy of Graphitic Carbon Nanomaterials Doped with Heteroatoms *Beilstein Journal of Nanotechnology* 6 2015: pp. 177 – 192. https://doi.org/10.3762/bjnano.6.17
27. **Moosburger-Will, J., Jäger, J., Strauch, J., Bauer, M., Strobl, S., Linscheid, F.F., Horn, S.** Interphase Formation and Fiber Matrix Adhesion in Carbon Fiber Reinforced Epoxy Resin: Influence of Carbon Fiber Surface Chemistry *Composite Interfaces* 24 (7) 2017: pp. 691 – 710. https://doi.org/10.1080/09276440.2017.1310315
28. **Liu, X., Yang, C., Lu, Y.** Contrastive Study of Anodic Oxidation on Carbon Fibers and Graphite Fibers *Applied Surface Science* 258 (10) 2012: pp. 4268 – 4275. https://doi.org/10.1016/j.apsusc.2011.12.076
29. **Zhang, G., Xu, H., Zhu, Y., Yan, C., Liu, D., Chen, G., Xiao, Z.** Simultaneously Improving Interfacial Adhesion and Toughness of Carbon Fiber Reinforced Epoxy Composites by Grafting Polyethyleneimine on the Carbon Fiber Surface to Construct a Rigid-Flexible Interface *Polymer Composites* 45 (13) 2024: pp. 12044 – 12056. https://doi.org/10.1002/pc.28617
30. **Wu, Y., Lu, H., Qin, F., Yang, S., Xu, P., Peng, H.X.** Establishing Interphase With "Rigid-Flexible Coupling" Crosslinked Network by Supramolecular Structure to Improve Interfacial Properties of High-Modulus Carbon Fiber Composites *Composites Part B: Engineering* 291 2025: pp. 111968. https://doi.org/10.1016/j.compositesb.2024.111968
31. **Tan, Y., Liu, J., Li, Y., Wang, Q., Zhou, W., Ao, Y., Li, M.** Constructing a New Multiscale "Soft-Rigid-Soft" Interfacial Structure at the Interphase to Improve the Interfacial Performance of Carbon Fiber Reinforced Polymer Composites *Composites Science and Technology* 248 2024: pp. 110458. https://doi.org/10.1016/j.compscitech.2024.110458
32. **Okuda, H., Young, R.J., Wolverson, D., Tanaka, F., Yamamoto, G., Okabe, T.** Investigating Nanostructures in Carbon Fibres Using Raman Spectroscopy *Carbon* 130 2018: pp. 178 – 184. https://doi.org/10.1016/j.carbon.2017.12.050
33. **Lu, J., Li, W., Kang, H., Feng, L., Xu, J., Liu, R.** Microstructure and Properties of Polyacrylonitrile Based Carbon Fibers *Polymer Testing* 81 2020: pp. 106267. https://doi.org/10.1016/j.polymertesting.2019.106267



© Zhang et al. *2026* Open Access This article is distributed under the terms of the Creative Commons Attribution 4.0 International License (http://creativecommons.org/licenses/by/4.0/), which permits unrestricted use, distribution, and reproduction in any medium, provided you give appropriate credit to the original author(s) and the source, provide a link to the Creative Commons license, and indicate if changes were made.